

## Article

# Investigations on the Adhesive Contact Behaviors between a Viscoelastic Stamp and a Transferred Element in Microtransfer Printing

Ling Jiang, Mengjie Wu, Qiuping Yu \*, Yuxia Shan and Yuyan Zhang 

College of Mechanical and Electronic Engineering, Nanjing Forestry University, Nanjing 210037, China; jiangl@njfu.edu.cn (L.J.); wumengjie@njfu.edu.cn (M.W.); yuxia@njfu.edu.cn (Y.S.); yuyan\_zhang@njfu.edu.cn (Y.Z.)

\* Correspondence: yuqiuping03@njfu.edu.cn

**Abstract:** Microtransfer printing is a sophisticated technique for the heterogeneous integration of separately fabricated micro/nano-elements into functional systems by virtue of an elastomeric stamp. One important factor influencing the capability of this technique depends on the adhesion between the viscoelastic stamp and the transferred element. To provide theoretical guidance for the control of adhesion in the transfer printing process, a finite element model for the viscoelastic adhesive contact between a polydimethylsiloxane (PDMS) stamp and a spherical transferred element was established, in which the adhesive interaction was modeled by the Lennard-Jones surface force law. Effects of the unloading velocity, preload, and thermodynamic work of adhesion on the adhesion strength, characterized by the pull-off force, were examined for a loading-dwelling-unloading history. Simulation results showed that the unloading path deviated from the loading path due to the viscoelastic property of the PDMS stamp. The pull-off force increased with the unloading velocity, and the increasing ratio was large at first and then became low. Furthermore, the influence of the preload on increasing the pull-off force was more significant under larger unloading velocity than that under smaller unloading velocity. In addition, the pull-off force increased remarkably with the thermodynamic work of adhesion at a fixed maximum approach.

**Keywords:** microtransfer printing; viscoelasticity; adhesive contact



**Citation:** Jiang, L.; Wu, M.; Yu, Q.; Shan, Y.; Zhang, Y. Investigations on the Adhesive Contact Behaviors between a Viscoelastic Stamp and a Transferred Element in Microtransfer Printing. *Coatings* **2021**, *11*, 1201. <https://doi.org/10.3390/coatings11101201>

Academic Editor: Alexander D. Modestov

Received: 1 September 2021  
Accepted: 27 September 2021  
Published: 30 September 2021

**Publisher's Note:** MDPI stays neutral with regard to jurisdictional claims in published maps and institutional affiliations.



**Copyright:** © 2021 by the authors. Licensee MDPI, Basel, Switzerland. This article is an open access article distributed under the terms and conditions of the Creative Commons Attribution (CC BY) license (<https://creativecommons.org/licenses/by/4.0/>).

## 1. Introduction

Microtransfer printing is an advanced technique in the area of material assembly and micro/nano manufacturing, which relies on the interfacial adhesion for integrating functional devices by transferring prefabricated micro/nano-elements from the growth substrate to the receiver substrate via a viscoelastic stamp [1]. As this technique does not require any specially designed adhesive layers or surface chemistries [2], it has broad application prospects in the fields of electronics, photonics [1], materials science [3] and bioengineering [4]. For example, it can be used to design skin-like biosensor system for noninvasive flexible electronic devices [5]; or for use in creating inhibitor film that controls and guides the initial corrosion attack effectively in materials science [3]; or through application in point-of-care devices or organs-on-chips in the field of bioengineering [4], and so on. However, the control of transfer printing, which includes the pickup process and the printing process, is still troublesome in actual operations due to the particular material characteristics of the stamp and the diversity of the transferred elements [6].

Polydimethylsiloxane (PDMS) is a widely used material for the stamp. It behaves as a transparent elastomer in solid state, but its predecessor is mixed with two viscous liquids, namely the base polymer and the curing agent. On one hand, this material owns both the elasticity of a solid and the viscosity of a liquid, that is the viscoelastic property. Due to this property, the viscoelastic material is sensitive to changes in its pulling velocity and

preload [2,7,8] and, as a result, the reasonable control of these two parameters becomes one of the difficulties in improving the transfer printing yield. On the other hand, the mixing ratio of the base polymer to the curing agent during preparation of PDMS has a significant effect on its work of adhesion [9]. The work of adhesion plays an important role in the contact mechanics of PDMS [10], and its influence on the performance of transfer printing cannot be ignored. To solve these problems, the mechanical behaviors and key parameters involved in the transfer printing process were extensively studied. For example, Cheng et al. [11] established a plane-strain viscoelastic model for the delamination of the stamp/transferred element interface using the energy method and analytically derived a relationship between the pull-off force and the pulling velocity of the stamp. In this model, the strength of interfacial adhesion was characterized by the pull-off force, which denoted the force required to separate the stamp and the transferred element, and the viscoelastic constitutive relation of the stamp was described by the Prony series. Feng et al. [12] investigated the critical pulling velocity of the stamp governing the pickup and printing processes based on the beam theory, in which the influence of the viscoelastic property of the stamp was reflected by a power-law expression relating the critical energy release rate to the pulling velocity. Liang et al. [13] proposed an analytical model for illustrating the dependence of the pull-off force under the plane-strain condition on the preload of the stamp using the fracture mechanics-based approach. The results showed that the preload would affect the stress at the stamp/transferred element interface and thus resulted in the increase of the pull-off force.

The above studies provide useful guidance for the control of pulling velocity and preload in actual transfer printing operations for films. However, for spherical transferred elements, which are often involved in micro-assembly [14], the interfacial mechanical behaviors during transfer printing are lacking in terms of systematic investigation. Furthermore, the effects of work of adhesion on the transfer printing mechanics are also unclear. To solve these problems, this work was undertaken to establish a viscoelastic adhesive contact model between an elastomeric PDMS stamp and a spherical transferred element, and to realize the quantitative prediction of the interfacial adhesion. The influences of the pulling velocity, preload, and work of adhesion on the strength of interfacial adhesion were demonstrated so that theoretical foundations can be provided for the control of parameters involved in the transfer printing process.

## 2. Model

A schematic representation of the contact between a viscoelastic stamp and a spherical transferred element is shown in Figure 1a. For the convenience of analysis, the following simplifications were made: (1) the stamp and the transferred element were turned upside down, the bottom of the stamp was fixed, and the transferred element was moved toward and then away from the stamp under a specific speed so that the effect of the pulling velocity in transfer printing can be investigated through changing the unloading velocity; (2) the transferred element was much stiffer than the stamp, and thus it can be approximated as a rigid body; and (3) the contact between the stamp and the transferred element can be analyzed through an axisymmetric model considering the axial symmetry of the spherical transferred element. The simplified model is illustrated in Figure 1b, in which  $R$  is the radius of the spherical transferred element,  $z(r)$  denotes the surface separation between the stamp and the transferred element at the radial distance  $r$  and can be expressed as,

$$z(r) = -\delta + w(r) + u(r) \quad (1)$$

where  $\delta$  is the approach between the bottom of the transferred element and the surface of the undeformed stamp, which is negative when the transferred element is above the undeformed stamp and otherwise positive. The  $w(r)$  represents the spherical spacing caused by the curvature of the transferred element and is given by  $w(r) = R - (R^2 - r^2)^{1/2}$ . While  $u(r)$  denotes the deformation on the surface of the stamp, which depends on the viscoelastic property of the stamp and the interfacial adhesion.

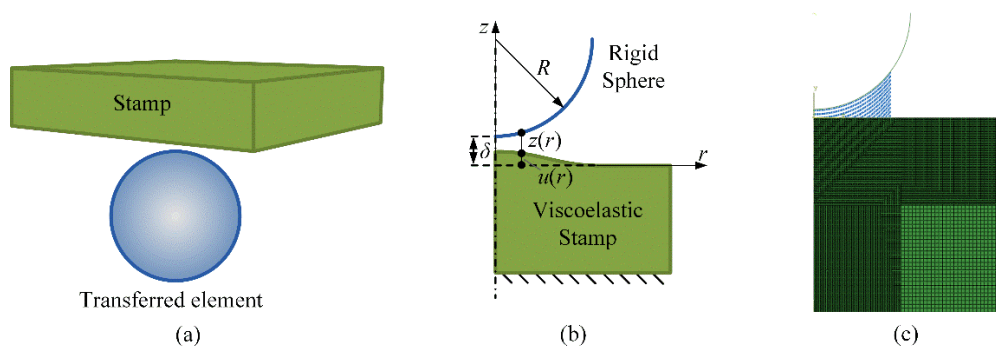


**Figure 1.** Schematics of the contact model between a viscoelastic stamp and a spherical transferred element. (a) three-dimensional model; (b) reduced axisymmetric model; (c) finite element model.

In microtransfer printing, which does not involve electrostatic interaction and liquid environment, the interfacial adhesion is mainly induced by the van der Waals interaction [15,16]. Based on the Derjaguin approximation [17], the van der Waals adhesion between the stamp and the transferred element can be characterized by the Lennard-Jones surface force law, which is expressed as [18]:

$$p(r) = \frac{8\Delta\gamma}{3z_0} \left\{ \left[ \frac{z_0}{z(r)} \right]^3 - \left[ \frac{z_0}{z(r)} \right]^9 \right\} \quad (2)$$

where  $p(r)$  is the pressure distribution on the surface of the stamp,  $\Delta\gamma$  denotes the thermodynamic work of adhesion, and  $z_0$  represents the surface distance at equilibrium.

The total force between the stamp and the transferred element can be given by:

$$F = - \int_{\Omega} p(r) dr \quad (3)$$

where  $\Omega$  is the calculation domain.

Positive values of  $F$  correspond to the repulsive force, while negative values correspond to the attractive force. The maximum value of the attractive force during the unloading stage is referred to as the pull-off force and denoted as  $F_{\text{pull-off}}$ , which is often utilized to characterize the strength of adhesion [19].

In order to solve the above axisymmetric viscoelastic adhesive contact problem, a finite element model, shown in Figure 1c, was established using the commercial Abaqus package. The transferred element was modeled as an axisymmetric discrete rigid, and the stamp was modeled with axisymmetric four-node elements. The material properties of the stamp were governed by the hyperelastic constitutive model, which was characterized by the Mooney-Rivlin strain energy function and the viscoelastic constitutive model characterized by the Prony series. The surface interaction between the transferred element and the stamp was simulated by the axial connector elements with nonlinear properties governed by the force-distance relation in Equation (2). Details about the simulation method can be found in references [20,21]. Considering that the van der Waals force decreases rapidly with the increase of distance, the axial connector elements were distributed only in the area close to the axis of symmetry ( $r = 0$ ). The nodes at the bottom boundary of the stamp and those at the axis of symmetry were constrained against displacement in  $z$  and  $r$  directions. The contact and separation processes between the stamp and the transferred element were simulated by the displacement control approach.

### 3. Results and Discussion

#### 3.1. Model Validation

The establishment of the viscoelastic adhesive contact model mainly involved two problems, that is: the characterization of the viscoelastic property of the stamp and the description of the interfacial adhesion. As a validation, the present simulation results were compared with Song's results [21] for the elastic adhesive contact problem and Chen's results [22] for the viscoelastic non-adhesive contact problem. As depicted in

Figure 2, good agreements between the present results and Song's results were achieved in terms of the variations of the dimensionless pull-off force with the Tabor parameter for the elastic adhesive contact problem, and the relative error between them was less than 1%, which validates the present description of the interfacial adhesion. Figure 3 shows the force-approach curve for the non-adhesive contact between a rigid sphere and a viscoelastic polymethylmethacrylate (PMMA) substrate, the creep function of PMMA was  $\varphi_c(t) = 7.0 \times 10^{-4} - 6.17 \times 10^{-5} \exp(-0.1t) - 8.38 \times 10^{-5} \exp(-7.47 \times 10^{-3}t)$ , (1/MPa), in which  $F_m$  is the peak load and  $\delta_0$  is the approach for the Hertzian contact at the peak load. Related conditions, including the radius of the sphere, the viscoelastic parameters of PMMA, and the loading history, were set to be the same as Chen's case [22]. Favorable comparisons between present results and Chen's results illustrate the correctness of the present model in characterizing the viscoelastic property of polymer-based materials.

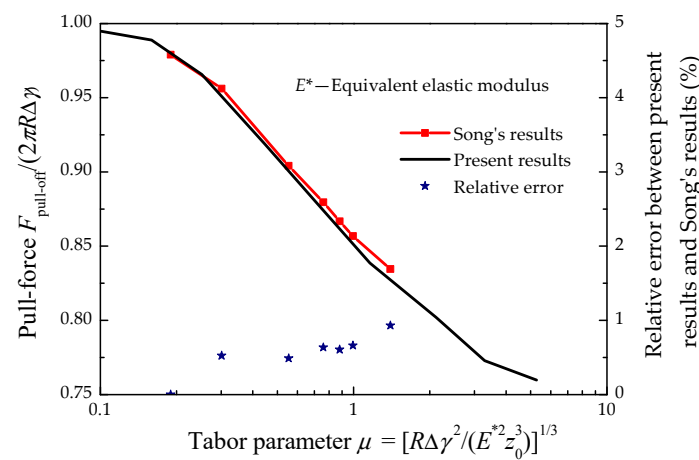


**Figure 2.** Comparison of the present numerical results with those of Song's [21] for the elastic adhesive contact problem.

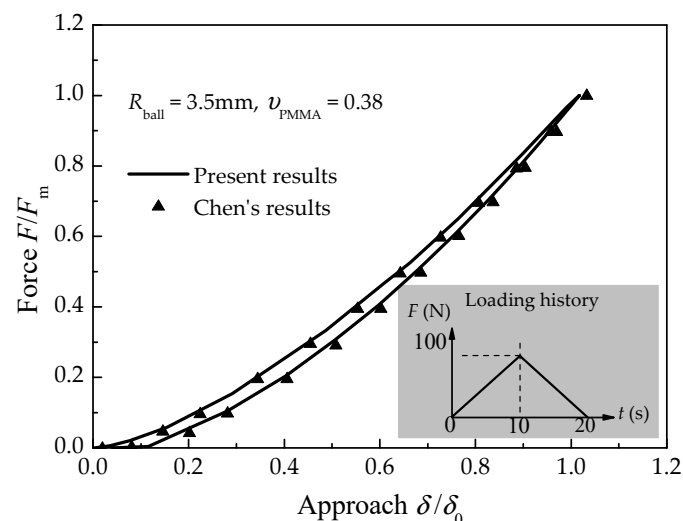


**Figure 3.** Comparison of the present numerical results with those of Chen's [22] for the viscoelastic non-adhesive contact problem.

### 3.2. Adhesive Contact Behaviors between a Polydimethylsiloxane Stamp and a Spherical Transferred Element

Finite element results of the adhesive contact between a PDMS stamp and a spherical transferred element, considering the effects of unloading velocity, preload, and work of adhesion, are presented in this section. According to the actual transfer printing process, the displacement history in the present analysis was set to follow a loading-dwelling-

unloading profile, shown in Figure 4, which means that the transferred element was moved downward to make contact with the PDMS stamp at a constant loading velocity until reaching a preset maximum approach, dwelling for a few seconds, and then retracting it at a prescribed unloading velocity. The force corresponding to the maximum approach  $\delta_{\max}$  is called the preload and denoted as  $F_{\text{preload}}$ . The radius  $R$  of the spherical transferred element was  $5 \mu\text{m}$ , the equilibrium distance  $z_0$  was  $0.044 \mu\text{m}$ , the loading velocity was  $1 \mu\text{m/s}$ , and the dwell time was  $2 \text{ s}$ . The material parameters of the PDMS related with the hyperelastic property were  $C_{10} = 0.178 \text{ MPa}$ ,  $C_{01} = 0.045 \text{ MPa}$ , and  $D_1 = 0.179 \text{ MPa}$  [11], and those related with the viscoelastic property were  $g_1 = 0.665$ ,  $g_2 = 0.05$ ,  $\tau_1 = 1.5$ , and  $\tau_2 = 10$  [23]. In order to make the results more generalizable, we transformed all the dimensional parameters into dimensionless ones. The dimensionless forms were referred to those proposed by Lin et al. [24], that is,  $F = F/(3\pi R\Delta\gamma)$ ,  $\delta = [3\pi^2\Delta\gamma^2R/(2E_\infty^*)]^{-1/3}\delta$ ,  $t = t/\tau_1$ ,  $\Delta\gamma = \Delta\gamma/\Delta\gamma_f$ , and thus  $v_{\text{unload}} = \tau_1 [3\pi^2\Delta\gamma^2R/(2E_\infty^*)]^{-1/3}v_{\text{unload}}$ ,  $E_\infty^*$  is the effective long-time relaxation modulus and satisfies  $E_\infty^* = E_\infty/(1-\nu^2)$ ,  $\nu$  is the Poisson's ratio of the stamp, which is set as  $0.48$  in the present analysis,  $\tau_1$  is the first relaxation time of the stamp material, and  $\Delta\gamma_f$  is the reference work of adhesion, which was chosen as  $\Delta\gamma_f = 1 \text{ J/m}^2$ .

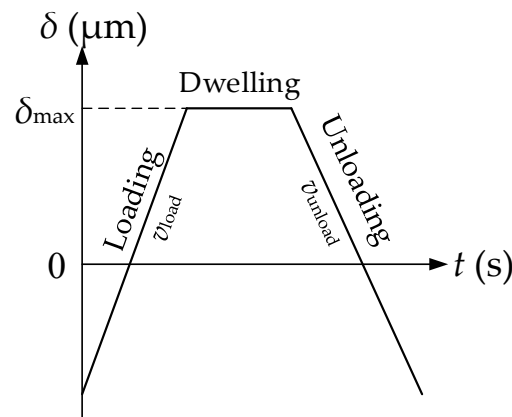
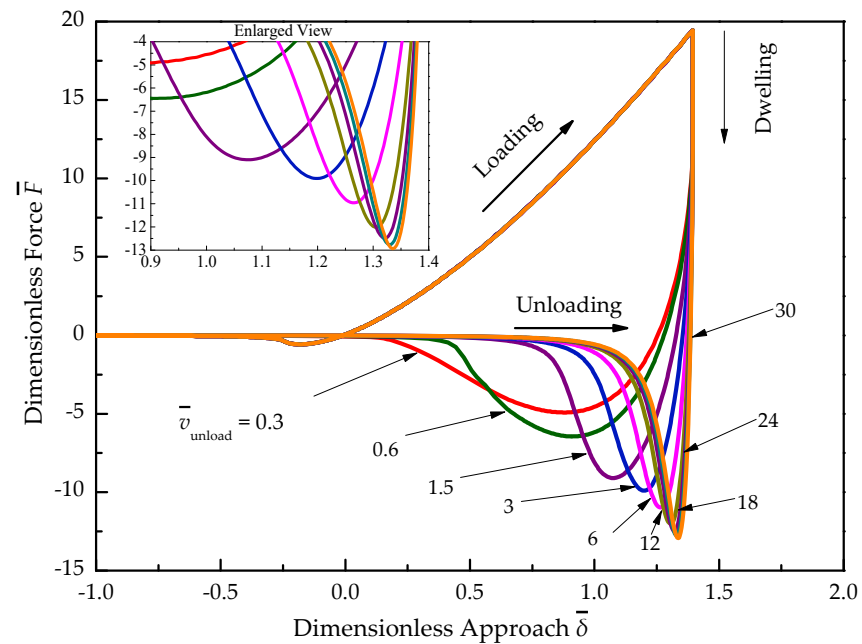


Figure 4. Loading history in the simulation.

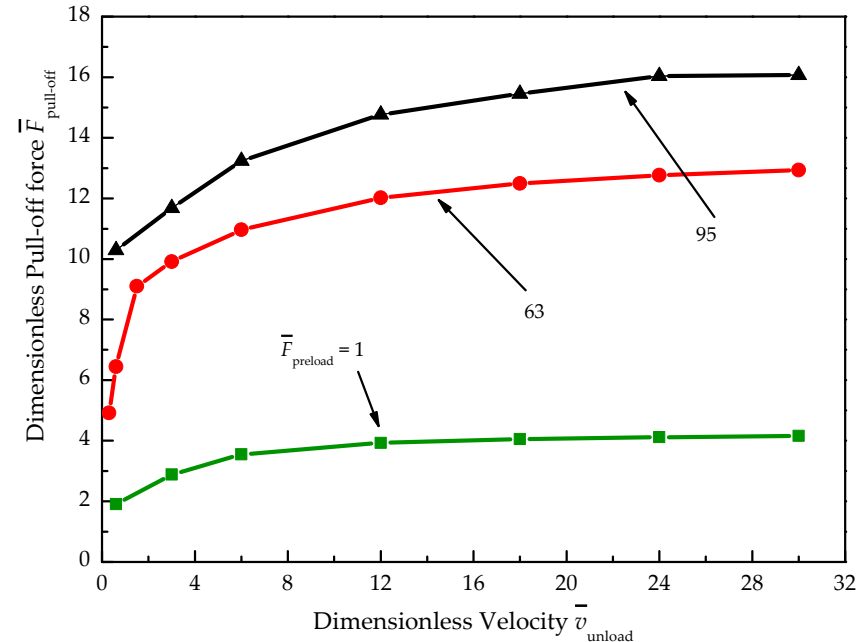
### 3.2.1. The Effect of Unloading Velocity

Figure 5 presents variations of force with approach under different unloading velocities. It can be seen that during the loading process, the transferred element experienced a weak attractive force from the stamp when the approach was small. As the approach increased, the attractive force increased first, then decreased, and eventually became the repulsive force. During the dwelling process, the force decreased rapidly, although the approach remained constant, which reflects the stress relaxation behavior of the viscoelastic stamp [25]. In addition, the force-approach curve during unloading did not coincide with that during loading due to the viscoelastic energy dissipation [26] in the separation of the transferred element from the stamp. Moreover, the unloading path deviated from each other for different unloading velocities. This can be attributed to the predominant viscous response at lower unloading velocities and the predominant elastic response at higher unloading velocities [26]. The difference in the viscous response and the elastic response resulted in the difference of energy required to promote interface delamination. Specific pull-off forces are shown in the enlarged view. To illustrate the influence of unloading velocity on the adhesion strength, Figure 6 shows changes of the pull-off force with the unloading velocity. As can be seen, for  $\Delta\gamma = 0.05$  and  $F_{\text{preload}} = 19$ , when the unloading velocity  $v_{\text{unload}}$  increased from  $0.3$  to  $30$ , the pull-off force increased about  $1.44$  times. However, when the unloading velocity  $v_{\text{unload}}$  was larger than  $12$ , increases of the pull-off force became insignificant. This implies that the adhesion interaction between the stamp and the transferred element can only be strengthened by increasing the unloading velocity in

a certain range during the pickup process in transfer printing, while it can be weakened through decreasing the unloading velocity during the printing process.



**Figure 5.** Force-approach curves for different unloading velocities under the condition of  $\Delta\gamma = 0.05$  and  $F_{\text{preload}} = 19$ .



**Figure 6.** The effect of unloading velocity on pull-off force under the condition of  $\Delta\gamma = 0.05$ .

### 3.2.2. The Effect of Preload

The effects of the preload on the adhesive contact behaviors can be interpreted in light of the loading-unloading curves shown in Figure 7. Although the loading paths overlap, the unloading paths demonstrated conspicuous dependence on the preload. This was due to the increasing residual viscoelastic deformations with the preload and the resultant larger residual interference between the stamp and the transferred element. Figure 8 illustrates variations of the pull-off force with the preload for three different unloading

velocities. It clearly shows the increase of the pull-off force with the preload, which was associated with the larger residual deformation and interaction area in larger preloads. Furthermore, the influence of the preload on the pull-off force was more significant under larger unloading velocity than that under smaller unloading velocity. The above results suggest that the combination of large preload and high unloading velocity was beneficial to the pickup process and adverse to the printing process.

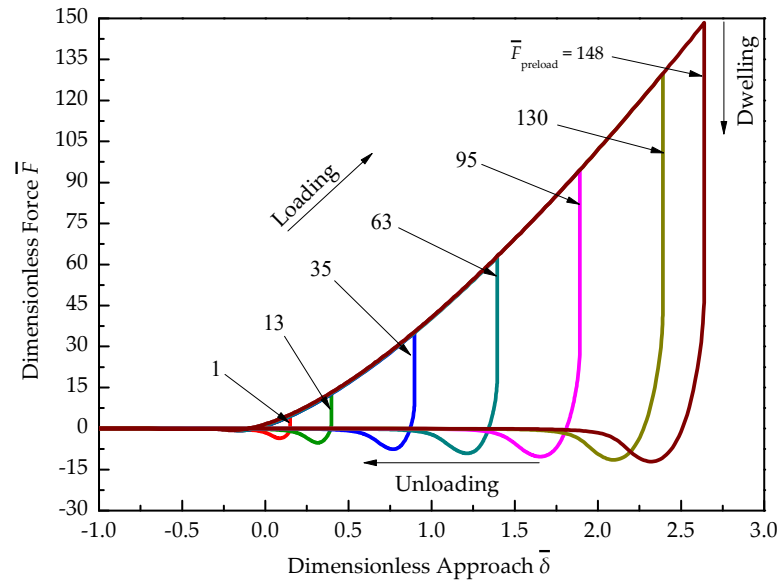


**Figure 7.** Force-approach curves for different preloads under the condition of  $\Delta\gamma = 0.05$  and  $v_{\text{unload}} = 0.6$ .

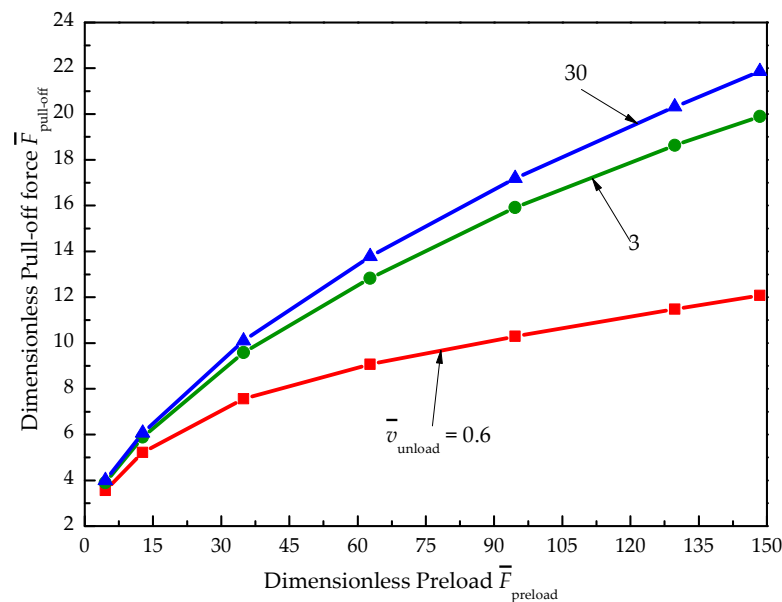
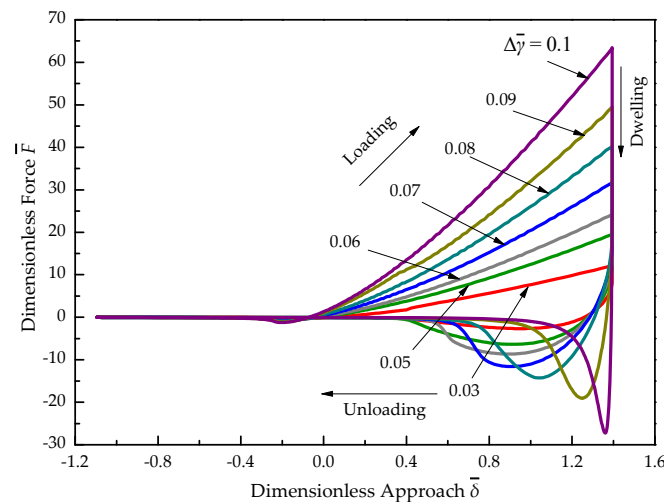


**Figure 8.** The effect of preload on pull-off force under the condition of  $\Delta\gamma = 0.05$ .

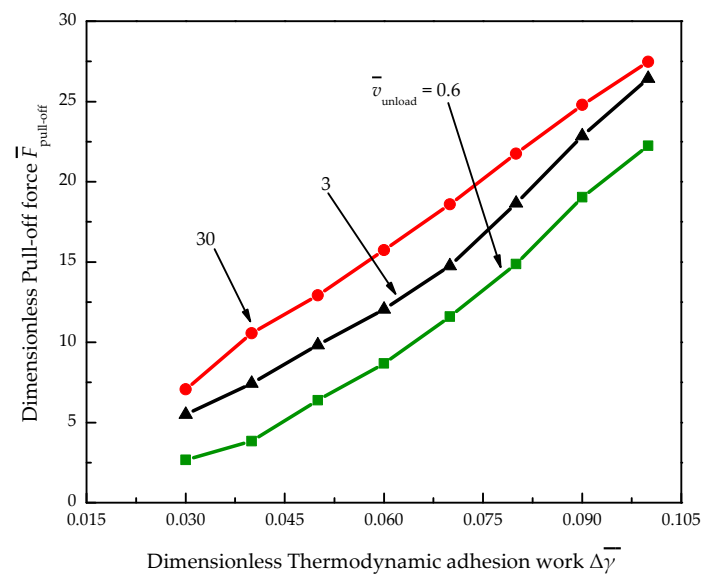
### 3.2.3. The Effect of Thermodynamic Work of Adhesion

Figure 9 presents effects of the thermodynamic work of adhesion on the interaction force between the stamp and the transferred element, while maintaining the same maximum approach. It can be seen that both the loading curve and the unloading curve were affected by the work of adhesion, and the distinction between the loading and unloading curves was more noticeable for a larger work of adhesion. The results of the various unloading velocities with pull-off force at different work of adhesion values are given in

Figure 10. Obvious increases of the pull-off force with increasing work of adhesion can be found. This behavior was related with the viscoelastic energy dissipation during unloading. As Nikkhah et al. [26] demonstrated, the dissipation energy, which was required for delaminating the viscoelastic adhesive interface, depended on the thermodynamic work of adhesion. Therefore, the larger the work of adhesion, the more difficult for the interface delamination, and the larger the pull-off force. Due to the fact that the adhesion between the stamp and the transferred element needs to be strong in the pickup process and weak in the printing process, the stamp should be properly designed so that its thermodynamic work of adhesion can satisfy the demand in both pickup and printing processes.



**Figure 9.** Force-approach curves for different thermodynamic work of adhesion under the condition of  $\delta_{\max} = 2.49$  and  $v_{\text{unload}} = 0.6$ .



**Figure 10.** The effect of thermodynamic adhesion work on pull-off force under the condition of  $\delta_{\max} = 2.49$ .

#### 4. Conclusions

A finite element model of a PDMS stamp and a spherical transferred element, considering the viscoelastic property of the stamp and the interfacial adhesion, was proposed to analyze the contact behaviors in transfer printing. The interfacial adhesion was simulated by the axial connector elements with nonlinear properties governed by the Lennard-Jones surface force law. This model was validated by the elastic adhesive contact model and

the viscoelastic non-adhesive contact model. In order to provide control strategies for the unloading velocity, preload, and the preparation technique of the stamp in actual transfer printing operations, which include the pickup and printing processes, a loading-dwelling-unloading history was applied to investigate the contact mechanics, and the pull-off force was utilized to represent the strength of adhesion. Main conclusions could be drawn as follows.

1. There were good agreements between the finite element results with those for the elastic adhesive contact problem and the viscoelastic non-adhesive contact problem, thereby validating the description of the interfacial adhesion and the characterization of the viscoelastic property of the stamp in the present model, respectively;
2. The force-approach curve during unloading did not coincide with that during loading due to the viscoelastic energy dissipation in the separation of the transferred element from the stamp. Furthermore, the unloading path deviated from each other for different unloading velocities and preloads;
3. The pull-off force between the stamp and the transferred element can only be enlarged by increasing the unloading velocity in a certain range during the pickup process, while it can be diminished through decreasing the unloading velocity during the printing process;
4. The pull-off force increased with the increasing preload, and the increasing ratio was higher under larger unloading velocity than that under smaller unloading velocity.
5. Both the loading curve and the unloading curve were affected by the thermodynamic work of adhesion, and the larger the work of adhesion, the more noticeable the distinction between the loading and unloading curves. The pull-off force increased remarkably with the thermodynamic work of adhesion at fixed maximum approach.

**Author Contributions:** Conceptualization, Y.Z.; funding acquisition, Y.Z.; project administration, Y.Z.; writing—original draft, L.J.; methodology, L.J.; writing—review & editing, M.W., Q.Y. and Y.S.; validation, M.W., Q.Y. and Y.S. All authors have read and agreed to the published version of the manuscript.

**Funding:** The authors would like to express their gratitude for the financial support received from the National Natural Science Foundation of China (no. 51805269) and the National Key R&D Program of China (2018YFB2000800).

**Institutional Review Board Statement:** Not applicable.

**Informed Consent Statement:** Not applicable.

**Data Availability Statement:** Data sharing is not applicable to this article.

**Conflicts of Interest:** The authors declare no conflict of interest.

## References

1. Zhou, H.; Qin, W.; Yu, Q.; Cheng, H.; Yu, X.; Wu, H. Transfer Printing and Its Applications in Flexible Electronic Devices. *Nanomaterials* **2019**, *9*, 283. [[CrossRef](#)]
2. Meitl, M.A.; Zhu, Z.T.; Kumar, V.; Lee, K.J.; Feng, X.; Huang, Y.Y.; Adesida, I.; Nuzzo, R.G.; Rogers, J.A. Transfer Printing by Kinetic Control of Adhesion to an Elastomeric Stamp. *Nat. Mater.* **2006**, *5*, 33–38. [[CrossRef](#)]
3. Neupane, S.; Rivas, N.A.; Losada-Pérez, P.; D’Haen, J.; Noei, H.; Keller, T.F.; Stierle, A.; Rudolph, M.; Terfort, A.; Bertran, O.; et al. A Model Study on Controlling Dealloying Corrosion Attack by Lateral Modification of Surfactant Inhibitors. *NPJ Mater. Degrad.* **2021**, *5*, 29. [[CrossRef](#)]
4. Martínez-Rivas, A.; González-Quijano, G.; Proa-Coronado, S.; Séverac, C.; Dague, E. Methods of Micropatterning and Manipulation of Cells for Biomedical Applications. *Micromachines* **2017**, *8*, 347. [[CrossRef](#)] [[PubMed](#)]
5. Chen, Y.; Lu, S.; Zhang, S.; Li, Y.; Qu, Z.; Chen, Y.; Lu, B.; Wang, X.; Feng, X. Skin-like Biosensor System via Electrochemical Channels for Noninvasive Blood Glucose Monitoring. *Sci. Adv.* **2017**, *3*, e1701629. [[CrossRef](#)] [[PubMed](#)]
6. Peng, P.; Wu, K.; Lv, L.; Guo, C.F.; Wu, Z. One-Step Selective Adhesive Transfer Printing for Scalable Fabrication of Stretchable Electronics. *Adv. Mater. Technol.* **2018**, *3*, 1700264. [[CrossRef](#)]
7. Jin, C.; Qiao, Q. Deformation of Pyramidal PDMS Stamps During Microcontact Printing. *J. Appl. Mech.* **2016**, *83*, 071011. [[CrossRef](#)]

8. Xu, Y.; Xu, Z.D.; Guo, Y.Q.; Dong, Y.; Ge, T.; Xu, C. Tests and Modeling of Viscoelastic Damper Considering Microstructures and Displacement Amplitude Influence. *J. Eng. Mech.* **2019**, *145*, 04019108. [[CrossRef](#)]
9. Yu, H.; Li, Z.; Jane Wang, Q. Viscoelastic-Adhesive Contact Modeling: Application to the Characterization of the Viscoelastic Behavior of Materials. *Mech. Mater.* **2013**, *60*, 55–65. [[CrossRef](#)]
10. Carrillo, F.; Gupta, S.; Balooch, M.; Marshall, S.J.; Marshall, G.W.; Pruitt, L.; Puttlitz, C.M. Erratum: “Nanoindentation of Polydimethylsiloxane Elastomers: Effect of Crosslinking, Work of Adhesion, and Fluid Environment on Elastic Modulus. *J. Mater. Res.* **2006**, *21*, 535–537. [[CrossRef](#)]
11. Cheng, H.; Li, M.; Wu, J.; Carlson, A.; Kim, S.; Huang, Y.; Kang, Z.; Hwang, K.C.; Rogers, J.A. A Viscoelastic Model for the Rate Effect in Transfer Printing. *J. Appl. Mech.* **2013**, *80*, 041019. [[CrossRef](#)]
12. Feng, X.; Cheng, H.; Bowen, A.M.; Carlson, A.W.; Nuzzo, R.G.; Rogers, J.A. A Finite-Deformation Mechanics Theory for Kinetically Controlled Transfer Printing. *J. Appl. Mech.* **2013**, *80*, 061023. [[CrossRef](#)]
13. Liang, C.; Wang, F.; Huo, Z.; Shi, B.; Tian, Y.; Zhao, X.; Zhang, D. Pull-off Force Modeling and Experimental Study of PDMS Stamp Considering Preload in Micro Transfer Printing. *Int. J. Solids Struct.* **2020**, *193–194*, 134–140. [[CrossRef](#)]
14. Sun, L.; Wang, L.; Rong, W.; Chen, L. Considering Van Der Waals Forces in Micromanipulation Design. In Proceedings of the 2007 International Conference on Mechatronics and Automation, Harbin, China, 5–8 August 2007; IEEE: Piscataway, NJ, USA, 2007; pp. 2507–2512.
15. Hsia, K.J.; Huang, Y.; Menard, E.; Park, J.U.; Zhou, W.; Rogers, J.; Fulton, J.M. Collapse of Stamps for Soft Lithography Due to Interfacial Adhesion. *Appl. Phys. Lett.* **2005**, *86*, 154106. [[CrossRef](#)]
16. Zhang, Y.; Wang, X.; Tu, Q.; Sun, J.; Ma, C. Mechanical Modeling and Characteristic Study for the Adhesive Contact of Elastic Layered Media. *J. Phys. Appl. Phys.* **2017**, *50*, 475601. [[CrossRef](#)]
17. Derjaguin, V.B. Theorie des Anhaftens kleiner Teilchen. *Prog. Surf. Sci.* **1992**, *40*, 6–15. [[CrossRef](#)]
18. Muller, V.M. On the Influence of Molecular Forces on the Deformation of an Elastic Sphere and Its Sticking to a Rigid Plane. *J. Colloid Interface Sci.* **1980**, *77*, 11. [[CrossRef](#)]
19. Zhang, Y.; Si, L.; Zhang, X.; Li, J.; Wang, W. Investigations of the Adhesive Contact Behavior of Elastic Layered Media with Surface Roughness. *J. Tribol.* **2019**, *141*, 044504. [[CrossRef](#)]
20. Kadin, Y.; Kligerman, Y.; Etsion, I. Loading–Unloading of an Elastic–Plastic Adhesive Spherical Microcontact. *J. Colloid Interface Sci.* **2008**, *321*, 242–250. [[CrossRef](#)] [[PubMed](#)]
21. Song, Z.; Komvopoulos, K. Adhesion-Induced Instabilities in Elastic and Elastic–Plastic Contacts during Single and Repetitive Normal Loading. *J. Mech. Phys. Solids* **2011**, *59*, 884–897. [[CrossRef](#)]
22. Wayne Chen, W.; Jane Wang, Q.; Huan, Z.; Luo, X. Semi-Analytical Viscoelastic Contact Modeling of Polymer-Based Materials. *J. Tribol.* **2011**, *133*, 041404. [[CrossRef](#)]
23. Kim, K.S.; Lin, Z.; Shrotriya, P.; Sundararajan, S.; Zou, Q. Iterative Control Approach to High-Speed Force-Distance Curve Measurement Using AFM: Time-Dependent Response of PDMS Example. *Ultramicroscopy* **2008**, *108*, 911–920. [[CrossRef](#)] [[PubMed](#)]
24. Lin, Y.-Y.; Hui, C.Y. Mechanics of Contact and Adhesion between Viscoelastic Spheres: An Analysis of Hysteresis during Loading and Unloading. *J. Polym. Sci. B Polym. Phys.* **2002**, *40*, 772–793. [[CrossRef](#)]
25. Gai, P.; Xu, Z.D.; Guo, Y.; Dai, J. Gradient Chain Structure Model for Characterizing Frequency Dependence of Viscoelastic Materials. *J. Eng. Mech.* **2020**, *146*, 04020094. [[CrossRef](#)]
26. Javan Nikkhah, S.; Moghbeli, M.R.; Hashemianzadeh, S.M. A Quantitative Correlation between Polyethylene/Graphene Interfacial Viscoelastic Dissipation and Deformation Parameters: A Molecular Simulation Study. *Int. J. Adhes. Adhes.* **2018**, *84*, 54–62. [[CrossRef](#)]